BLDC motor analysis in software ANSYS Electronics

Jakub Eichler[1*] and Tomáš Zvolský[2]

[1] Institute of Mechatronics and Computer Engineering, Technical University of Liberec, Czech Republic
[2] Department of Vehicles, Technical University of Liberec, Czech Republic
jakub.eichler@tul.cz

Abstract. The BLDC motor design is currently greatly simplified by the use of FEM software. This article deals with the possibilities of realizing such a design in the ansys electronics software.

Keywords: BLDC motor, ansys electronics and simulation of motoin

1 INTRODUCTION

Because first electric vehicle is more then 100 years older, is problem of electric drive very actual. Main parts of production of BLDC (Brushless DC electric motor) motors are produced in China. In this time, when is global trade difficult, is know how about construction of BLDC motor in Europe guarantee of independence. The aim of this study is to find out the possibilities of the design environment ansys electronics 2019.

2 MATERIALS AND METHODS

The BLDC motor, like all motors, works on the Lorentz force principle. This force is converted into torque in the air gap thanks to the bonds in the bearings. In terms of electrical properties of the source, the topology of the control circuit for simulations is designed in the circuit design software ansys elelctronics.

One of the basic parameters of a BLDC motor is its power, or the torque it exerts on the shaft. In Ansys software, the moment is calculated from the forces acting on each element in the volume according to the equation [1]

$$F_{\alpha} = \sum_{\beta} \int_{V} \frac{\partial}{\partial x_{\beta}} T_{\alpha\beta} d^3 x \quad . \tag{1}$$

For the simulation, the RMxprt module is used first, which tries to design a motor with the highest possible performance with the given parameters. The design is based on analytical equations, so it is very fast, but it does not take into account a significant part

M. Petr et al. (eds.), *62nd International Conference of Machine Design Departments (ICMD 2022)*,
Atlantis Highlights in Engineering 28,
https://doi.org/10.2991/978-94-6463-423-5_5

of the events in the magnetic circuit and assumes that all magbetic induction flux will pass from the stator perpendicularly to the rotor.

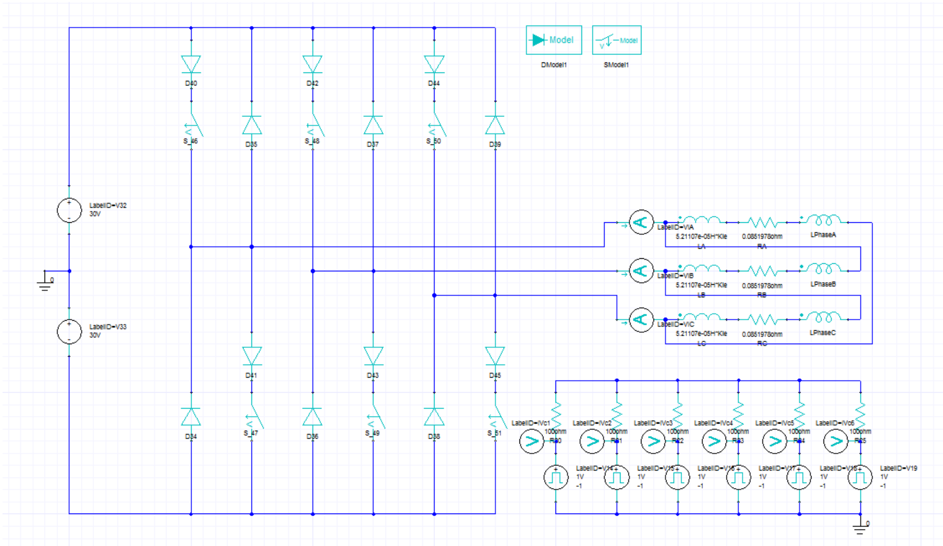

Fig 1. Topology of electrical circuit

As Figure 1 shows, the motor is powered by 30 V and is controlled by a 4 quadrant inverter. All important constraints such as transistor recovery times and on-state resistance are built into the software. The basis here is also the model of the winding, which is energized from the inverter. The winding is represented here by two coils and one resistor. Their values are determined by the RMxprt module itself. The coil is divided into two, the first is linear and the second from Maxwel 2D represents the magnetic circuit.

3 RESULTS AND DISCUSSION

Calculating in the Maxwell 2D module we get results that are much closer to the real engine than RMxprt. The FEM calculation is demanding on machine time and therefore only an eighth is calculated, which we can afford because the motor is symmetrical and contains 8 equal parts around the circumference. It is only necessary to set the boundary conditions on master and slave.

If the motor is running operating rotating and is loaded with a certain torque (in this particular case 900 rpm and 15 Nm), we get the result of the 3 following figures (FIG. 2-4). It can be seen from Figure 2 that for this condition (amplitudes) both the stator and the rotor are oversaturated in small areas.

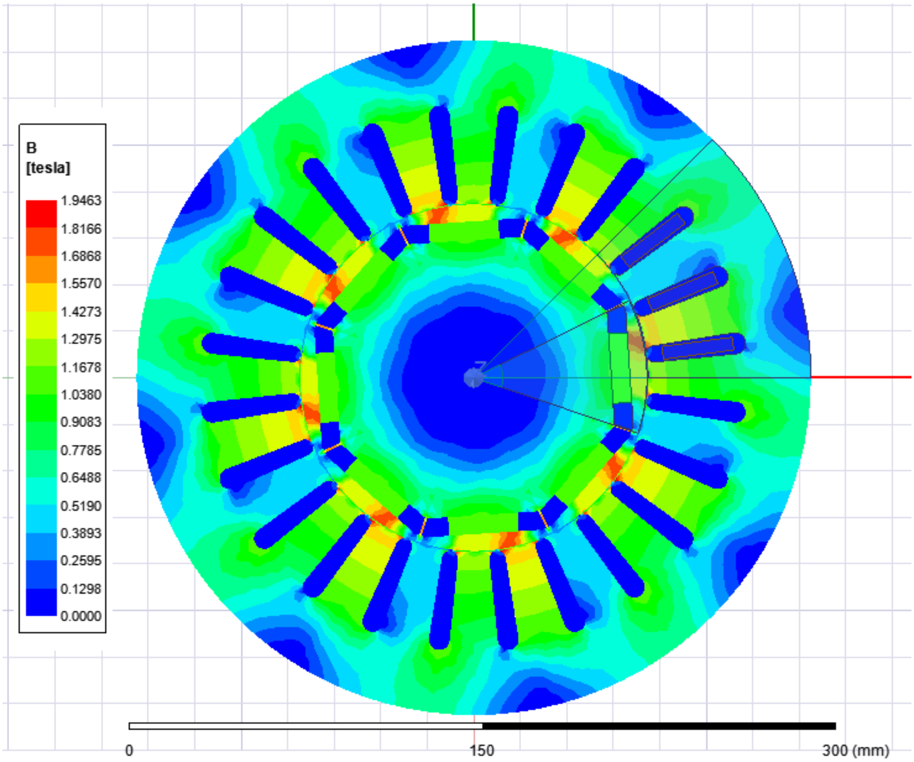

Fig.2 Flux density in motor - magnitude

Figure 3, which shows the magnetic induction vectors, gives us the information that the supersaturation is only in a small area around the winding slot. In addition, the direction in which the induction is issued here is not radial. The problem is that the software does not allow you to arbitrarily set the groove geometry. This groove shape has already been optimized for the minimum dimension of the groove end.

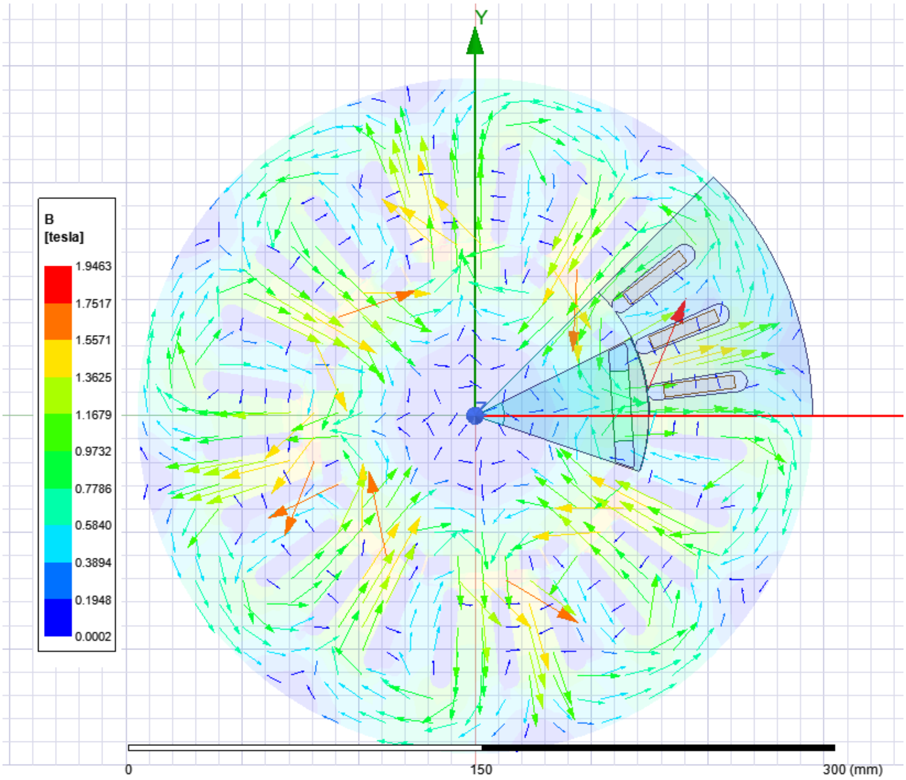

Fig. 3 Flux density in motor - vector flux

Figure 4 shows the current distribution in a section of the motor. The magnetic sheets, air gap and neodymium magnets are shown here in green. The green area has minimal (up to zero) current density. So we can say that current does not flow in this area. The windings in the stator were outlined in other colors. The cut is made in the "amplitude" time, but even so the current density achieved here is below 4 A/mm2. The maximum possible value for continuous operation is 5 A/mm2 due to Joule heat.

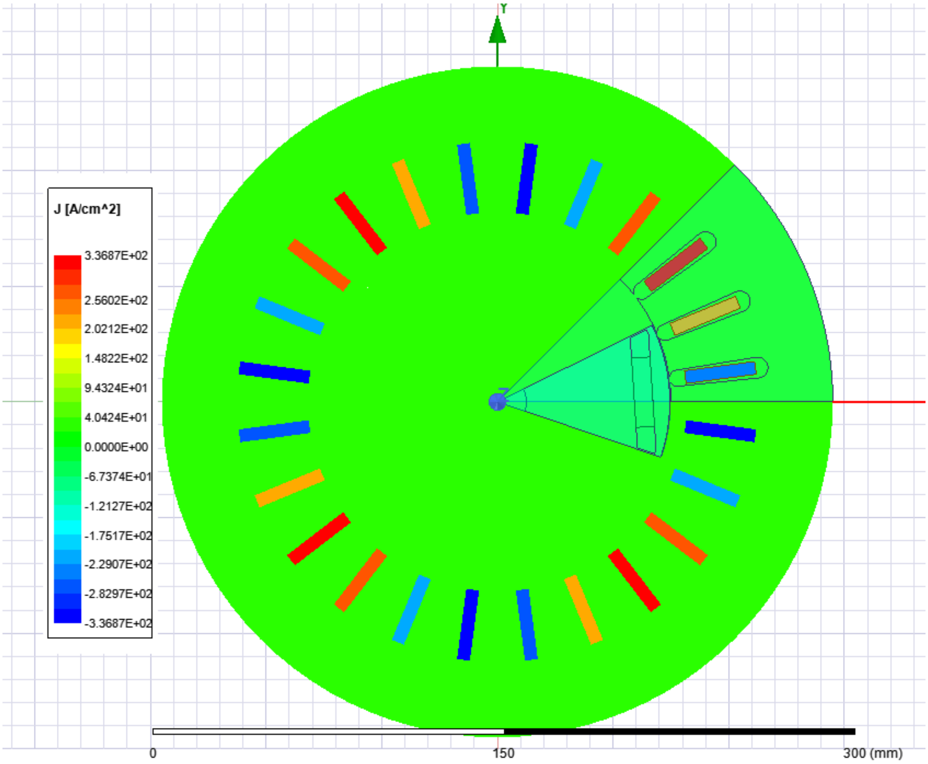

Fig.4 Current density in motor

For the simulation, the engine is loaded by the calander characteristic and of course also by its own moment of inertia. Starting from 0 to full speed is required. The speed dependence graph at start-up is in Figure 5.

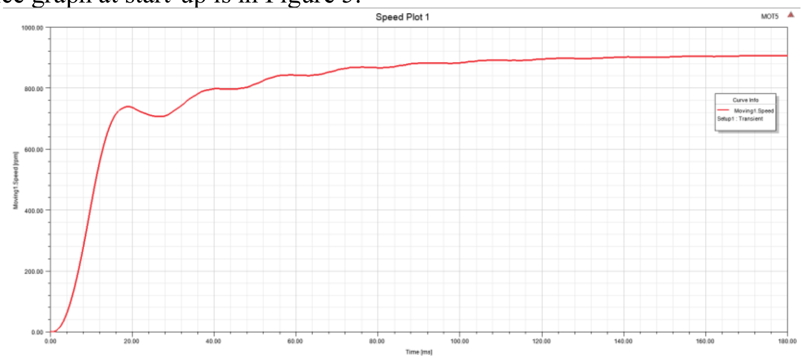

Fig.5 Motor speed - calender characteristics

As shown in Figure 5, the takt motor starts up after approx. 150 ms to an operating speed of approx. 900 RPM.

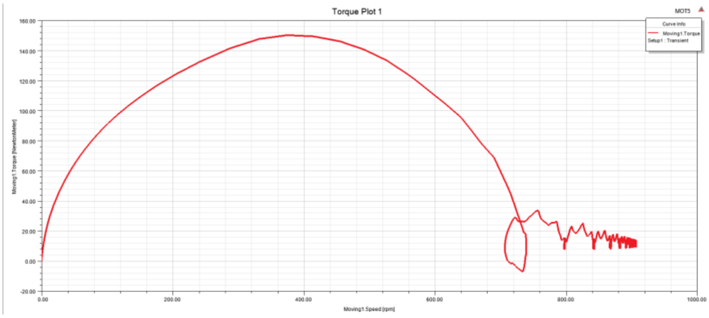

Fig. 6 Kvasi Torgue charakteristic

Figure 6 shows the obtained torque characteristic, which was obtained by plotting the dalambert torque as a function of speed from the engine start-up data.

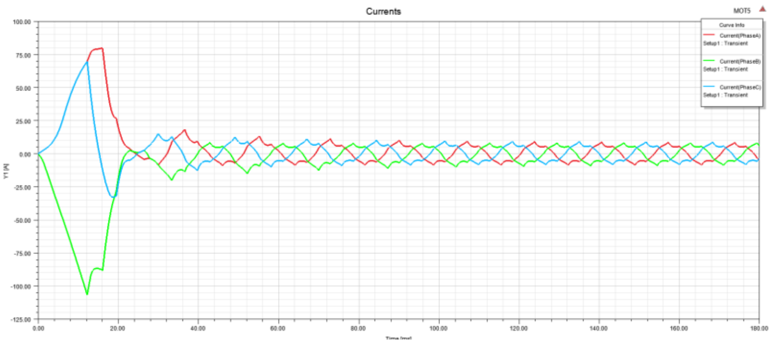

Fig.7 Currents in stator winding

Figures 7 and 8 describe what happens in the winding. As can be seen from Figure 7, there is a significant current peak of about 80 A when the motor starts up, while after starting up to the rated speed the current is about 10 A. However, what is more interesting is what happens in the voltage, where 300 V should be induced, as Figure 8 suggests, which does not quite correspond to the supply voltage, which is ten times lower, but same problem have not another autors [2,3]. With a suitable design, after a few iterations, the flow of the current was smoother than the authors indicate in the publications [4,5]

Fig. 8 Induced voltage in windings

4 CONCLUSIONS

It was possible to design a BLDC motor for several iterations, which has operating processes in its stator and rotor within limits where it is not saturated with magnetic induction and current density. The actual construction of the engine has not yet taken place due to time constraints.

ACKNOWLEDGEMENTS

The result was obtained through the financial support of the European Union in the frames of the project “Modular platform for autonomous chassis of specialized electric vehicles for freight and equipment transportation”, Reg. No. CZ.02:1:01=0:0=0:0=16 025=0007293:
This work was partly supported by the Student Grant Competition of the Technical University of Liberec under the project No. SGS-2022-3084.

REFERENCES

1. Maxwell Help Release 2019 R2 April 2019, distributed in software.
2. M. M.K, G. S. Warrier, P. Pathivil, S. Kanagalakshmi and R. Archana, "Design and Performance Analysis of Brushless DC Motor Using ANSYS Maxwell," 2019 2nd International Conference on Intelligent Computing, Instrumentation and Control Technologies (ICICICT), 2019, pp. 1049-1053, doi: 10.1109/ICICICT46008.2019.8993368.
3. O. Rahmani, M. Iltarabian and S. A. Sadrossadat, "Modeling and Simulation of Speed and Efficiency of BLDC Motor as A Starter Motor Based on Multilayer Perceptron (MLP) Neural Network," *2018 IEEE Transportation Electrification Conference and Expo, Asia-Pacific (ITEC Asia-Pacific)*, 2018, pp. 1-5, doi: 10.1109/ITEC-AP.2018.8433299.
4. N. N. Bobe and V. S. Rajguru, "120 kW BLDC Motor Design for Electric Train Application using ANSYS Maxwell," *2022 IEEE 19th India Council International Conference (INDICON)*, Kochi, India, 2022, pp. 1-5, doi: 10.1109/INDICON56171.2022.10039947.
5. S. V. Patil and R. Saxena, "“Design & Simulation of Brushless DC Motor Using ANSYS for EV Application”," *2022 IEEE International Students' Conference on Electrical, Electronics and Computer Science (SCEECS)*, BHOPAL, India, 2022, pp. 1-5, doi: 10.1109/SCEECS54111.2022.9740973.